Journal of Catalysis 280 (2011) iii–vi

Contents lists available at ScienceDirect

Journal of Catalysis

journal homepage: www.elsevier.com/locate/jcat

Journal of Catalysis Vol. 280, Issue 2, 2011

Contents

PRIORITY COMMUNICATION

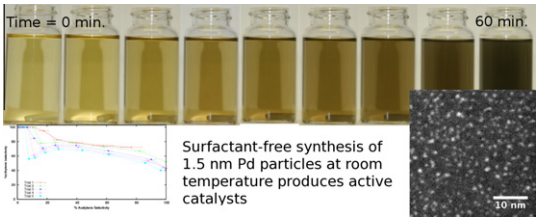

A simple route is described for the preparation of Pd nanoparticles via reduction of $Pd(OAC)_2$ by methanol at room temperature, without the need for any capping agents. These catalysts do not require pretreatment and exhibit high selectivity for the hydrogenation of acetylene to ethylene.

REGULAR ARTICLES

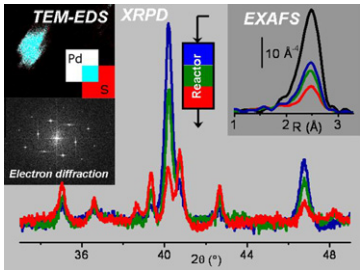

Palladium on carbon catalysts for the purification of terephthalic acid are shown to deactivate by sintering and sulfur and lead poisoning.

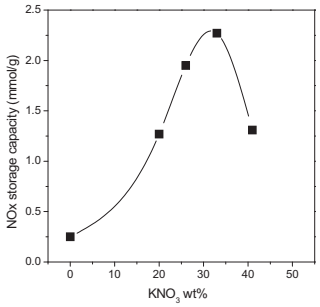

A novel catalyst with the composition of Pt–KNO_3 supported on potassium titanate nanobelt has been investigated for NO_x storage/reduction at 350 °C. High NO_x storage capacity with the optimal adding amount of KNO_3 as 26–33 wt.% has been revealed.

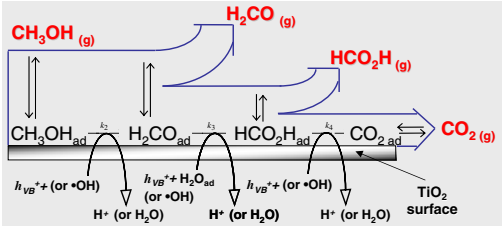

The photo-steam reforming reaction of methanol, yielding H_2 and CO_2 together with formaldehyde and formic acid as oxidation intermediates, proceeds through a hydroxyl radical-mediated indirect path and a direct, hole-mediated path. Water molecules on the photocatalyst surface assist proton transfer to noble metal nanoparticles, where H_2 is produced.

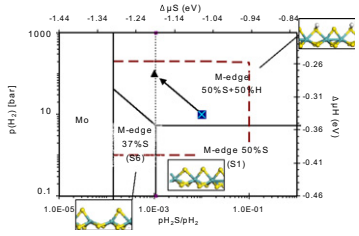

Surface phase diagrams for MoS_2 M- and S-edges are revisited on the basis of DFT calculations including for the first time entropic and enthalpic vibrational corrections to electronic energies. Free-energy barriers along edge reduction pathways are reported.

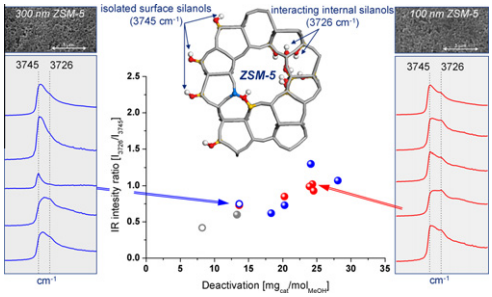

Internal framework defects are crucial for the deactivation behaviour of the ZSM-5 catalysts in the conversion of methanol to hydrocarbons. While the activity is related to the acid site density, the deactivation rate correlates with the measured intensity ratio of the IR bands for internal silanols at 3726 cm^{-1} and for external silanol groups at 3745 cm^{-1} (I_{3726}/I_{3745}).

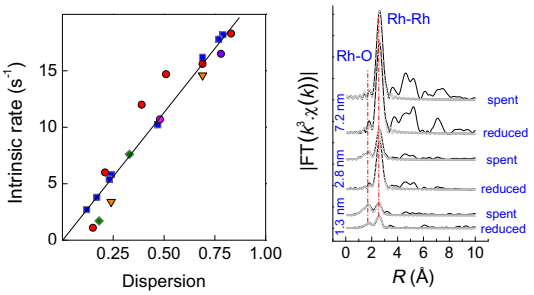

The intrinsic rate for steam methane reforming of Rh increases linearly with metal dispersion independent of the support (CeO_2, $CeZrO_2$, ZrO_2, SiO_2) when corrected for the amount of non-nonreducible Rh. CH_4 activation is rate limiting under typical steam reforming conditions. At a temperature of 500 °C catalysts containing very small Rh metal particles deactivate due to oxidation of the metal phase.

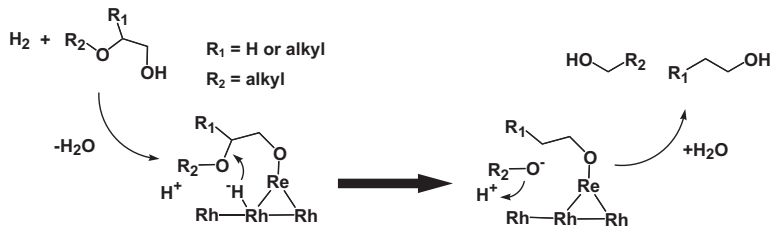

High activity and regioselectivity in hydrogenolysis of ether's C—O bond neighboring —CH_2OH group were achieved on Rh–ReO_x/SiO_2 catalyst through hydride → proton transfer mechanism.

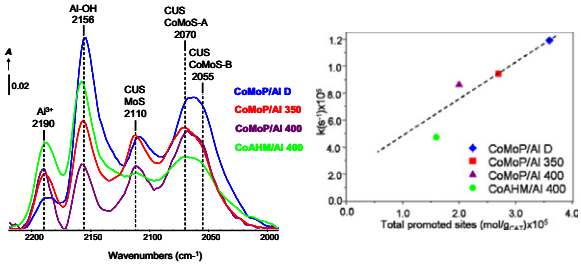

The number of Co-promoted sites in CoMoP/Al_2O_3 HDS catalyst prepared with $Co_{7/2}PMo_{12}O_{40}$ depends on the pretreatment given to the catalyst before its activation (sulfidation). Two different types of promoted CoMoS sites with different HDS intrinsic activities seem to co-exist in the sulfided catalyst.

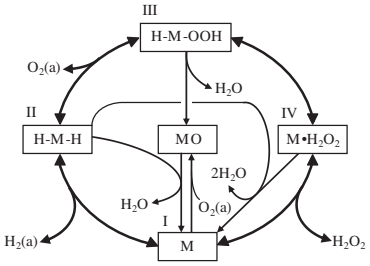

Kinetic analyses of the direct H_2O_2 synthesis from H_2 and O_2 and the H_2O_2 decomposition on Pd/C catalyst in water containing H^+ and Br^- ions and adsorption measurement of Br^- ion on the catalyst proposed a hydride-hydroperoxy species H-M-OOH (M represents the metal surface) to be the key intermediate in the H_2O_2 formation, the direct H_2O formation, and the H_2O_2 decomposition.

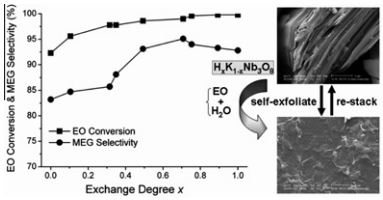

Layered niobic acids are reported as efficient catalysts for the selective hydration of ethylene oxide. The adjustable acidity and *in situ* self-exfoliation effect are crucial for the good catalytic performance.

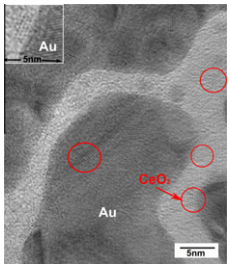

The catalytic CO oxidation ($2CO + O_2 \rightarrow 2CO_2$) was studied on Au islands/film decorated with ceria nanoparticles (<5 nm). Despite its relatively large grain size, the gold film was activated upon decorating its surface with ceria nanoparticles, showing a comparable activity to that reported for supported Au/TiO_2 and Au/CeO_x catalysts with gold particles of a few nanometers.

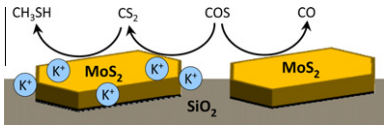

The synthesis of CH_3SH on K^+ promoted MoS_2/SiO_2 from COS and H_2 proceeds through the disproportionation of COS and the consecutive hydrogenation of CS_2 mainly on the K^+-MoS_2 phase. In parallel, COS is reduced to CO and H_2S on the unpromoted MoS_2 phase.

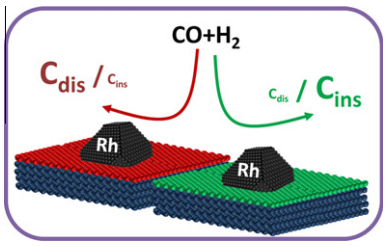

As ascertained using highly dispersed model $Rh/M@Al_2O_3$ catalysts, the selectivity pattern in the synthesis of oxygenates from synthesis gas is dictated by the electron-withdrawing/donating power (Lewis acidity/basicity) of the underlying metal oxide promoter.